Ain Shams Engineering Journal 14 (2023) 102231

Contents lists available at ScienceDirect

Ain Shams Engineering Journal

journal homepage: www.sciencedirect.com

Three-dimensional modeling and defect quantification of existing concrete bridges based on photogrammetry and computer aided design

Saleh Abu Dabous [a,b,*], Rami Al-Ruzouq [a,b], Daniel Llort [c]

[a] Department of Civil and Environmental Engineering, University of Sharjah, Sharjah, United Arab Emirates
[b] Sustainable Civil Infrastructure Systems Research Group, Research Institute of Sciences and Engineering, University of Sharjah, Sharjah, United Arab Emirates
[c] Ministry of Energy and Infrastructure, United Arab Emirates

ARTICLE INFO

Article history:
Received 3 May 2022
Revised 11 January 2023
Accepted 1 March 2023
Available online 16 March 2023

Keywords:
Bridge Failure
3D model
Close-range photogrammetry
Image processing
Defect quantification
Bridge Monitoring

ABSTRACT

Bridge infrastructure is aging and deteriorating and requires innovative condition monitoring and assessment to ensure safety and maintain serviceability. Current practices for bridge condition assessment depend mainly on visual inspection. Innovative data collection technologies can assist in bridge inspection and defect identification and circumvent the limitations of traditional visual inspection. This research aims to apply photogrammetry principles and image processing techniques to develop a full-scale three-dimensional (3D) bridge structure model for defect identification and quantification. The data source to establish the point cloud models is a set of digital images taken at the bridge site. The point cloud models are developed by analyzing high-resolution images captured using a Nikon D4S camera. The images are captured from different positions/locations to provide extensive stereo coverage and maximum overlapping. Two hundred images of the bridge are processed with PhotoModeler software along with the calibration information, and ground control points (GCPs) coordinates to create the models. A standard digital close-range image processing is implemented to generate the 3D points cloud model. The calibration and orientation processes are made over a deformed situation. However, the developed CAD bridge drawings depict the original undeformed geometry. The extracted bridge inventory data from the 3D model, including bridge geometry information and bridge damage quantification, can provide a baseline for the bridge monitoring system to detect bridge deterioration over the years. The developed photogrammetric 3D model has an RMSE of 0.0081 m and uncertainty of ± 0.0041 m. Future research can aim at developing reusable parametric objects for bridges in Revit and coding scripts using programming languages such as Dynamo or Python to perform further analysis of the captured information.

1. Introduction

Bridges are critical assets in today's infrastructure as they link roads and highways, providing commuters and cargo transporters with essential mobility services. They require regular inspection and maintenance to provide adequate and safe service. Bridge infrastructure is considered unsatisfactory when they sustain excessive structural degradation due to material deterioration caused by several factors, including harsh environment, traffic collisions, and increasing traffic volume and load [1]. In addition, structural and functional degradation may occur due to under design of structures, lack of quality control during construction, issues with material durability, and insufficient rehabilitation and maintenance actions. The US Department of Transportation reported that around 23% of the in-service 612,000 bridges need to be revised or updated [2]. It is observed that bridges could deteriorate years earlier than their expected lifespan [3]. Hence, it is vital to develop and use systems to update bridge inventory information, which will help develop accurate bridge deterioration models to forecast future bridge maintenance and repair requirements.

Current bridge condition assessment and inspection practices rely primarily on visual inspection [4–6]. In the US, bridge inspection and condition assessment guidelines are developed and regulated by the Federal Highway Administration (FHWA) and the American Association of State Highway and Transportation Offi-

* Corresponding author at: Department of Civil and Environmental Engineering, University of Sharjah, Sharjah, United Arab Emirates.
E-mail address: sabudabous@sharjah.ac.ae (S. Abu Dabous).

https://doi.org/10.1016/j.asej.2023.102231
2090-4479/

cials (AASHTO) [7,8]. Results from these inspections are documented in the National Bridge Inventory (NBI) system, then used to model bridges' conditions and develop their rating [9]. The inspection is typically conducted by a certified bridge inspector visiting the structure to assess the conditions of the bridge elements based on their external appearance and using standard testing tools. It is essential to exploit modern technologies capable of modeling the bridge structure and producing a full-scale computer representation to measure defects and deterioration to overcome the challenges traditional bridge inspection strategies present. It will control costs and simultaneously provide excellent-quality data [10,11]. Light Detection and Ranging (LiDAR) is one data collection technology based on laser scanning, which has the potential to reconstruct three-dimensional (3D) models using dense and accurate point clouds [12,13]. It facilitates rapid and accurate spatial data collection and hence, is widely used in the field of civil engineering, including structural health monitoring [12–14], road defect detection [15], highway safety [16], and 3D reconstruction [15,16]. Another feasible alternative is photogrammetry, commonly utilized for mapping and surface reconstruction [17]. It has various applications, notably engineering, chemistry, and biomechanics. In civil engineering alone, applications necessitating the assessment of 3D structures and their changes are abundant [17,18]. It is often used to analyze the stability of road pavement under the force of braking vehicles, detect cracks in structures and measure their width, and determine bridge deformation, among other applications [19]. Over the last two decades, there has been rapid growth in digital imaging and computer systems.

Moreover, digital cameras and photogrammetry software interfaces have become economical for engineering requirements. Photogrammetry is the science of utilizing state-of-the-art techniques in processing multiple two-dimensional (2D) images to develop accurate 3D models with the capability of accurately measuring and analyzing ground truth information from 3D models [20]. Photogrammetry techniques have become a reliable alternative to traditional surveying and inspection activities, especially when large areas with complex geometric details are involved.

Previous studies have considered using photogrammetry for measurements and analysis related to bridge structures [21]. Hu et al. [22] proposed a framework methodology based on close-range photogrammetry (CRP) to monitor bridge deformation. The study combined image recognition technology, direct linear transformation, and collinear equations to calculate the deformation based on five sets of coordinates. Compared with the overall reading of the total station, the technique produced an error of less than 0.1 mm. Another study assessed the feasibility of measuring bridge deflections using CRP under different load scenarios [23]. The study on a 165 m long bridge reported that photogrammetry yielded higher accuracy than terrestrial laser scanning under dynamic loading scenarios. Belloni et al. [24] proposed a framework methodology for automatic crack monitoring utilizing photogrammetry and convolutional neural network. The study reported that the key sources of error were a result of misinterpretation of crack-like objects, namely, cables, wires, tile borders, etc. Another study developed a methodology to evaluate the quality of the digital point clouds generated based on data collected with Unmanned Aerial Vehicle (UAV) and Terrestrial Laser Scanning (TLS) techniques [25,26]. The methodology was evaluated on an existing Australian heritage bridge, comparing point cloud models generated from both methods in terms of points distribution, noise level, completeness of data, and surface and geometric precision. The results showed that the UAV photogrammetry has a better points density, more accurate measurements, and an acceptable level of outlier noise. In comparison, TLS generated a more accurate geometrical model with a high level of point density.

Although several studies have already investigated different photogrammetric and image processing methods to evaluate the existing condition of bridge structures, there is still a gap in considering the integration between these methods with other geometric modeling techniques using software such as AutoCAD and Revit. Therefore, this research aims to analyze the potential of applying photogrammetry principles and image processing techniques to develop a full-scale 3D model of bridge structures and investigate the possibility of using the developed model to measure and quantify defects of the structure. In addition, the research aims at extracting critical bridge inventory data from the 3D model, including bridge geometry information (surface-to-surface horizontal and vertical clearances, dimensions of structural members, and bridge drawings), bridge damage information (surface conditions and damage quantification), as well as the ability to initiate a bridge monitoring system to detect bridge deterioration over the years. State-of-the-art photogrammetry software (PhotoModeler Premium) and Computer-aided design (AutoCAD) software are utilized to build the 3D models. The results provide a full-scale modeling of the bridge structure to support engineers and inspectors in visualizing the structure and assessing the conditions of the different bridge components. These models are essential for the bridge management decision-making process.

2. Photogrammetric principles

Photogrammetry analyzes the collected 2D images of an object to determine its three-dimensional geometry, including its location, size, and shape. Photogrammetric methods can be classified into two types based on their data collection technique: aerial or terrestrial (close range) photogrammetry. In aerial photogrammetry, a high-resolution aircraft-mounted camera takes images vertically. Multiple and overlapping images are taken while the aircraft is flying along the flight path of the targeted site to ensure complete coverage [27]. On the other hand, in terrestrial photogrammetry, the data is collected within a close range (less than 100 m) of the targeted objects. Multiple images are taken from different positions and orientations with a handheld or fixed (on a tripod) camera. In this approach, two primary processes aid in translating 2D photographic information to 3D representation: interior and exterior orientation. 1) Interior orientation: This process involves restructuring the perspective system characterized by the internal geometry of the photographic equipment, utilizing the parameters acquired during the camera calibration procedure. These parameters include the focal length and position of the sensor's principal point, dimensions, and lens distortions [28]. Interior orientation helps to reduce the errors resulting from the operation of non-metric cameras. 2) Exterior orientation: During the 3D modeling phase, this process establishes the position of each camera relative to the ground when the photograph was taken. However, a minimum of one camera position must be available to determine the relative external orientation, which can be accomplished utilizing the position (X, Y, Z) and orientation (ω, φ, κ) parameters of other cameras. If there are not enough ground control points (GCPs), the system will initiate network adjustment, including relative and absolute orientation.

In contrast, relative orientation estimates the external orientation parameters of one image by utilizing another image in a different image coordinate system. Based on perspective geometry, the concurrent intersection of a minimum of five pairs of parallel rays dispersed within the model is necessary for the intersection of the remaining points. Analytical calculations help to determine the equations defining these rays. In contrast, the relative orientation parameters are estimated by utilizing co-planarity equations for every two images, which can be represented as follows [29]:

$$\begin{vmatrix} 1 & \frac{b_y}{b_x} & \frac{b_z}{b_x} \\ x_1 & y_1 & -f \\ x_2 & y_2 & z_2 \end{vmatrix} = 0, \quad (1)$$

where b_x, b_y, and b_z are respectively the spaces among the center of projection of two images for the X, Y, and Z axes, while (x_1, y_1, -f) are the coordinates of a point in the first image, known as the principal point and f is the focal length of the camera; (x_2, y_2, z_2) are the coordinates of a point in the second image and referred to them in the first image. The latter point is found from the point in the coordinate system of the second image (x'_2, y'_2, f) using both a translation and a rotation:

$$\begin{bmatrix} x_2 \\ y_2 \\ z_2 \end{bmatrix} = R. \begin{bmatrix} x'_2 \\ y'_2 \\ -f \end{bmatrix} + \begin{bmatrix} b_x \\ b_y \\ b_z \end{bmatrix}, \quad (2)$$

where R is the rotation matrix, defined by the following equation:

$$R = \begin{bmatrix} cos\varphi cos\kappa & sin\omega sin\varphi cos\kappa + cos\omega sin\kappa & -cos\omega sin\varphi cos\kappa + sin\omega sin\kappa \\ -cos\varphi sin\kappa & -sin\omega sin\varphi sin\kappa + cos\omega cos\kappa & cos\omega sin\varphi cos\kappa + sin\omega cos\kappa \\ sin\varphi & -sin\omega cos\varphi & cos\omega cos\varphi \end{bmatrix} \quad (3)$$

where (ω, φ, κ) represent rotation angles around the X, Y, and Z axes, respectively [23,30]. As per the collinearity model, when the relative position of the camera is solved, the camera station and the position of the image point on the bridge lie in a straight line.

Absolute orientation: This process facilitates model adaptation from the image coordinate system to the ground coordinate system utilizing GCPs to scale and locate the model. The scale factor can be determined by comparing the actual distances obtained during field measurement to those obtained from the model acquired after relative orientation. Rotating the model around the X- and Z-axes levels the model, rendering φ null in the rotation matrix. The transformation equation used to adapt the model to the real-world coordinate system is represented as shown below:

$$\begin{bmatrix} X \\ Y \\ Z \end{bmatrix} = k.R. \begin{bmatrix} x \\ y \\ z \end{bmatrix} + \begin{bmatrix} X_O u \\ Y_O \\ Z_O \end{bmatrix}, \quad (4)$$

where X_O, Y_O, and Z_O are the principal ground coordinates of the camera, k is the previously calculated factor; R is the matrix with φ and κ rotation angles obtained from the leveling stage of the model.

The camera calibration process estimates the deviation of the geometry of image formation in a real camera from the geometry of the central perspective projection, which arises from the limitations of the camera lens [31]. This process plays a vital role in photogrammetric object restitution. During calibration, metric cameras can precisely retrieve the principal point coordinates due to the embedded fiducial marks on their image plane. Conversely, non-metric cameras are made without this feature, making their interior orientation parameters unidentified and unstable. Semi-metric cameras are modified non-metric cameras adapted to improve the stability of the internal orientation elements and reduce the film deformation effects at the time of exposure. This process often uses a self-calibration approach that retrieves the essential distance, point, and lens distortion concurrently through the object reconstruction through a bundle adjustment based on the collinearity equations and additional correction functions. Bundle adjustment determines the interior and exterior orientation parameters and the 3D object coordinates [32].

3. Material and method

To serve the purpose of this research, a framework methodology based on CRP techniques and image-based modeling, illustrated in Fig. 1, is proposed and implemented. The framework consists of four main phases: (1) Site selection and field preliminary preparation: this includes target design and placement, camera configuration(s), and establishing instrument positions; (2) Data collection and image capturing: the images of the selected bridge are captured using digital camera, and terrestrial information were collected using total station and traditional terrestrial surveying techniques such as using theodolite, total station, or RTK GPS; (3) Photogrammetry Processing: process the collected data in a photogrammetric software such as PhotoModeler to retrieve a 3D point cloud bridge models that can be used in the production of full 3D geo-referenced textured bridge models, which is integrated into a computer-aided design (CAD) software for further processing; and (4) Bridge Information Modeling: generate a 3D bridge information model to extract the required information including geometric data, as-built/current drawings, surface conditions, and other structural information essential for populating bridge inventory data and condition information in Bridge Management Systems (BMS).

3.1. Site selection and field preparation

The bridge selected for the implementation of photogrammetric modeling is a reinforced concrete rigid frame highway bridge more than 35 years old. It is located on Interchange No. 6, Al Dhaid Road, Sharjah, United Arab Emirates (25° 18′ 06″ N latitude, and 55° 35′ 43″ E longitude). The selection was based on the condition and age of the bridge, as well as on the lack of availability of bridge drawings. This bridge carries the south and northbound traffic on I-6, including 4,500 trucks and heavy vehicles traversing through it daily. The superstructure consists of four girders and five-floor beams supporting a reinforced concrete deck with safety barrier railings on each side. Four columns and end abutments support the superstructure.

3.1.1. Target design

Photogrammetric software requires coded targets to distinguish them from the surrounding background and facilitate sub-pixel measurement [33]. Using a large number of well-distributed target points promotes higher accuracy when defining the absolute orientation (scaling and leveling) of the 3D bridge model. The minimum required size of the targets, T, can be estimated using a point-tracking technique and the following equation [34]:

$$T = \frac{D \cdot p}{f} \quad (7)$$

where D is the distance between the position of the camera and the targeted element, f is the focal length, and p is the pixel size [35]. The 3D coordinates of the target points (GCPs) can be obtained using GPS and the total station. In addition to their utilization in the definition of model orientation, this data can also be utilized to estimate the accuracy of the generated 3D model by comparing it with the actual data determined by the total station. In this project, 113 high-contrast black and white circular targets (calculated size was 60 mm or 2.3622 in) were distributed throughout the bridge structure (refer to Fig. 2 A). Fifty-four (54) points were placed on the longitudinal girders, 32 on the columns, 18 on the cross girders, and nine on the bridge deck. The selected GCPs were evenly distributed at the outer edge of the bridge. Moreover, GCPs should consider the terrain differences in the landscape (points are set at the highest and lowest elevations). Moreover, the

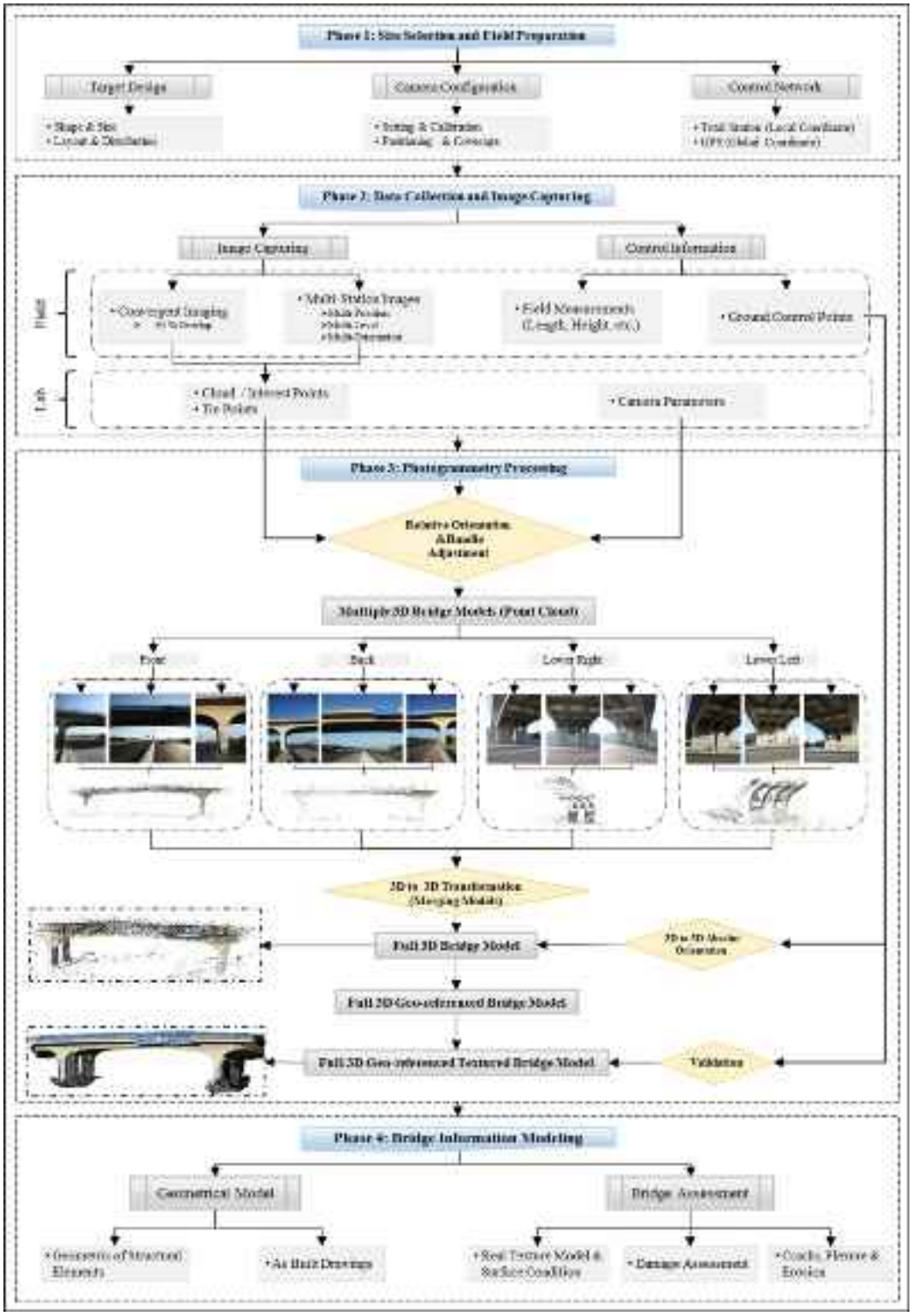

Fig. 1. Proposed framework for defect quantification.

distance between the nearest GCPs was between 2 m and 20 m. A sample of the target layouts distributed on the bottom deck and column of the bridge structure is illustrated in Fig. 2 B.

3.1.2. Camera configuration

The camera configuration, including the settings and the positioning, are critical factors that affect the development of an accurate bridge inventory. It is necessary to maintain simplicity and cost-effectiveness in the instrumentation to ease the difficulty entailed in this process. Although specifically produced for photogrammetric analysis, conventional metric cameras are costly. However, more recently, commercial off-the-shelf digital cameras provide enhanced ease of use and suitability for high-precision measurements due to improved image sensors and camera calibra-

Fig. 2. A) Artificial targets used for calibration and orientation and B) a sample of target layout on the bridge structure.

tion techniques [20]. In this research, the photogrammetric survey is accomplished using a Nikon D4S (shown in Fig. 3), a low-light hybrid single-lens reflex camera (HDSLR). The camera is equipped with a 16.2-megapixel FX-format CMOS image sensor. The AF NIKKOR 24 mm f/2.8D from Nikon provides a wide coverage area and is used for image capturing. The lens aperture is fixed at the highest f-stop setting (f/22), and the lens focus was set to ∞ improve the depth of coverage and enhance target detection. The camera is used in auto-exposure mode to augment exposure time. The setup included a tripod to prevent camera motion during image capture.

Once the camera settings are appropriately configured, the equipment must be calibrated for field use. Camera calibration is carried out in the laboratory at fixed parameters before data collection at the site. The PhotoModeler software includes a calibration module, and the procedure is executed by capturing numerous images of an array of flat target marks from various positions. Once the images are imported into the software, the photogrammetric module utilizes these calibration files to calculate the inner geometric camera parameters. These initial values are further refined during self-calibration with bundle adjustment. More details on the calibration process can be obtained in [28,36]. Table 1 illustrates the geometric parameters and the tangential and radial lens distortion coefficients obtained following camera calibration.

Table 1
Geometric parameters of Nikon D4S + 24 mm lens.

Parameter	Value	Deviation
Focal length (mm)	24.4876	0.001
Continuous speed (fps)	11	
Principal point position × (mm)	17.8412	0.001
Principal point position y (mm)	11.9562	0.001
Sensor width (mm) FX	35.9190	
Sensor height (mm) FX	23.9221	
Image Resolution [pixel]	3696 × 2456	
pixel size mm/pixel	0.0097	
K1 [-]	5.73E-05	
K2 [-]	1.64E-07	
K3 [-]	−2.10E-10	
P1 [-]	−1.27E-05	
P2 [-]	−1.01E-05	

3.1.3. Control network

The control network helps determine a photogrammetry project's reference coordinate system and scale. The conventional method involves surveying fixed GCPs using the total station to establish their 3D coordinates [28]. This project establishes an integrated network control involving GPS and the total station information. The signals collected by GPS receivers are utilized to calculate the exact location of features on the globe [20]. Trimble TSC3 controller and Trimble R10 GNSS 440 channels receiver are utilized in this research (Fig. 4 A). The receiver has a precision of ± 3 mm + 0.1 ppm RMS in the horizontal direction and ± 3.5 m m + 0.4 ppm RMS in the vertical direction during high-precision static surveying.

Furthermore, an operating range of up to 4 miles is achievable. The GPS is integrated with a Leica Builder 400 total station to survey the coordinates of GCPs distributed throughout the bridge infrastructure. The equipment has a long-range coverage capability of up to 1000 m; a dual-axis compensator; ± 3 mm + 2 ppm accuracy (with/without prism); 30X magnification; and 3″ angular accuracy. A circular level sensitivity of 6′/2 mm was utilized for this purpose. Fig. 4 A and B illustrate the control equipment used.

Fig. 3. Nikon D4S camera used for close-range photogrammetry.

3.2. Data collection

The data collection procedure is based on several factors, including determining the camera parameters based on the camera calibration, selecting the camera stations, defining a reference system, providing sufficient coverage and adequate exposure of the structure in the captured images, and providing sufficient data storage facilities [37].

3.2.1. Image acquisition

The triangulation principle states that an individual target must be captured in two images at least to obtain spatial information. However, improved results may be obtained using four or more images [33]. Due to the significant size of this bridge, the camera's field of view (FOV) does not encompass the complete bridge. Hence, it was divided into four smaller models (front side, backside, lower left, and lower right) to facilitate the data collection and ease the modeling process. A total of 250 high-resolution

Fig. 4. Trimble TSC 3 controller and Trimble R10 GNSS 440 channels receiver, and B) Leica Builder 400 total station for photogrammetry network control.

(3696 × 2456 pixels) images are captured from 11 different camera positions (from P1 to P11) to provide extensive coverage. The camera positions are well distributed: 3 on either side of the bridge length (P1 to P6) and four below the bridge's deck from P7 to P11 (Fig. 5). Each position includes at least three different camera levels: eye level, lower, and higher than eye level. In addition, images with different orientations are captured to provide maximum coverage and overlapping (at least 80 %) and maintain a convergent viewing angle of 90°, ensuring a minimum area of uncertainty. Fig. 5 B depicts a schematic of the camera positions and orientations utilized in this research. Fig. 6 (A and B) illustrates a sample of the images obtained using different camera orientations, different camera levels, and overlapping images when captured from position 1. During data collection, the distance between the camera stations and the bridge surface is maintained at 17.2850 m.

3.2.2. Control information

To accurately scale the 3D model generated by the photogrammetric software, it is necessary to obtain the actual dimensions of the bridge. High accuracy is achieved by surveying the coordinates of several GCPs distributed throughout the bridge infrastructure using total station and GPS. At the same time, the measurements are utilized to validate the results obtained after the 3D modeling. The integrated field surveying approach is expected to be a more accurate form of result validation than the conventional measurement techniques using tapes, plumb lines, or leveling staff. The procedure involves setting up GPS stations at two locations, in this case, at station P8 and Station P11, to determine their precise 3D coordinates. According to a static survey, data from the GPS reference station is received through a clipped-on controller. The GPS antenna lies collinear with the vertical axis of the total station. Once the antenna is connected to the total station, the coordinates obtained from the GPS reference station are initialized. Subsequently, these measurements are used to obtain the coordinates of the GCPs distributed on the bridge structure.

3.3. Photogrammetric processing

Following the data collection process, the images and the associated camera calibration file are uploaded to the photogrammetric software (PhotoModeler). Forty-five (45) overlapping images with 90° convergent angles were captured to model the front side of the bridge. The photogrammetric procedure models the ray geometry

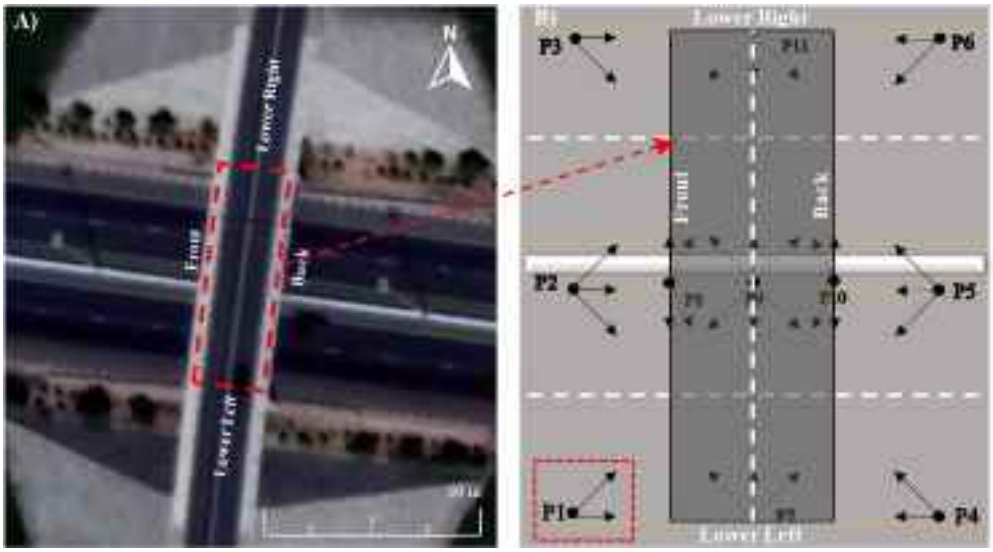

Fig. 5. Top view of a bridge section, B) schematic diagram of camera positions and orientations.

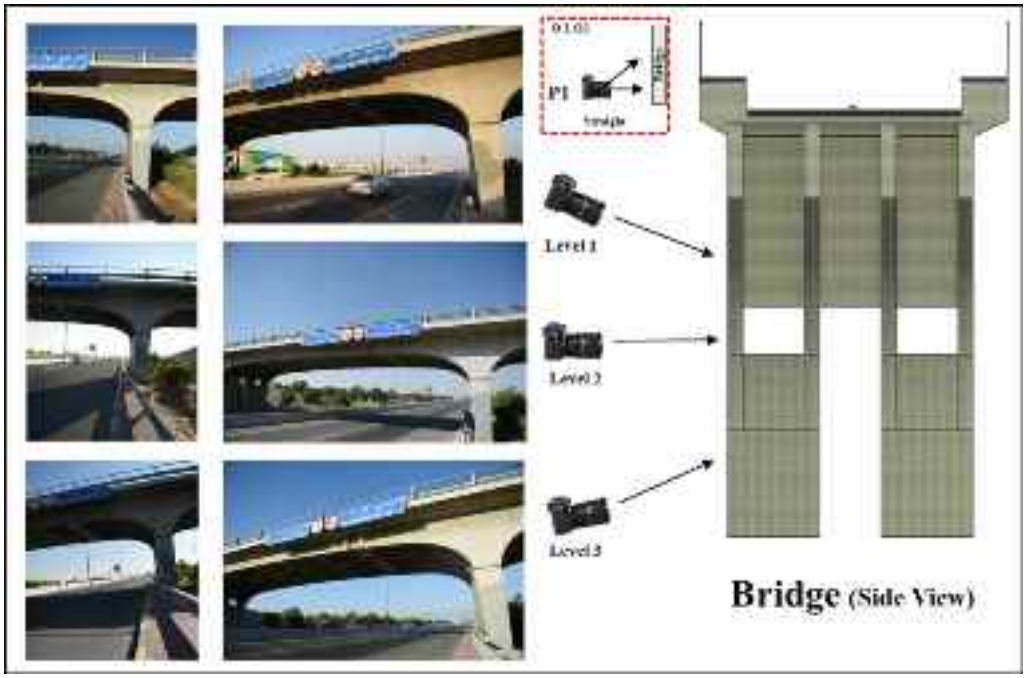

Fig. 6. Sample images captured from position 1 A) Straight Orientation, B) Inclined Orientation.

extracted from the images. Then, the imported images determine the 2D projections of the bridge points and the bridge's reference coordinate system. The subsequent step involves bundle adjustment, which aids in determining the image location and orientation within the reference system. This process is accomplished by defining a minimum of five tie-points between overlapping images, which generates a system of equations that will establish the relative external orientation between the images. The model for the front side included forty-one (41) tie points. Subsequently, 3D point clouds of the bridge model were obtained during the process of restitution. Fig. 7 A illustrates the 3D point clouds generated for the front-side model. Out of the forty-five (45) images, three (3) were discarded during the point cloud generation due to various errors during data collection, such as insufficient overlapping and inadequate feature detection resulting from sun glare. Around thirty (30) GCPs were used in the modeling process, ten (10) for the photogrammetry processing, and the rest to validate the model. Table 2 presents the model's exterior orientation parameters (EOPs) associated with a sample of ten (10) images. This table indicates the quality of the images utilized in the photogrammetric process. The precision of the X, Y, and Z coordinates lie between 4 and 9, 2 – 14, and 3 – 14 mm, respectively. The maximum residual reported was 2.10 pixels.

Like the front-side model, the remaining sections (back, lower left, and lower right sides) are developed (Fig. 7 B, C, and D), and the tie points are defined. Subsequently, these four (4) models are stitched together using tie points present in the convergent sections of each model to generate the 3D point clouds of the complete bridge structure (Fig. 7 E).

4. Results and discussion

The main objective of photogrammetric measurements is to reconstruct an object. Productive analyses can then be performed, mainly when these measurements are used to generate a complete 3D geo-referenced textured model. The primary output extracted from the photogrammetric modeling of the bridge infrastructure is highlighted in this section. This output comprises bridge inventory data, including geometric measurements of structural components, bridge drawings, vertical clearance measurements, and damage quantification. Typically, the photogrammetry model contains noise from the surroundings and background of the object. Therefore, all noise must be removed before the model can be used efficiently for bridge inspection. In this case, editing software such as AutoCAD and Revit, developed by Autodesk, removes all the surrounding and background noises from the bridge model. The complete model can be used in different applications, such as extracting the geometric model or assisting in the bridge assessment process.

4.1. Geometrical modeling

While PhotoModeler can extract 3D points from images, it is not easy to access, understand or use this information. These limitations have led to incorporation of other software such as AutoCAD and Revit. The final model will enable users to access the model easily and navigate quickly to find the required information. Moreover, it can be used as a database for the structure. The primary intent is to export the PhotoModeler model to AutoCAD to obtain the 3D geometrical information, which is then exported to Revit to include the texture and material details of the model.

Fig. 8 shows the transformation of the 3D models across the different software packages. The surface (texture) model visualizes the point clouds and lines that shape the structure. AutoCAD was used to transform the surface model into a schematic (wireframe) model. The schematic model can be a complete object representation using point clouds from PhotoModeler. Subsequently, Revit was utilized to develop the schematic model into a complete 3-D model. Finally, textures are added to each side of the bridge to obtain a realistic impression of the structure. Textures provide an authentic quality to the 3D model, making its replication of a real object more suitable for human perception and understanding. The final model (a Revit model) can be used to easily extract the bridge's structural and geometrical information, which makes the model amenable to better visualization and serves as the input for further 3D information extraction.

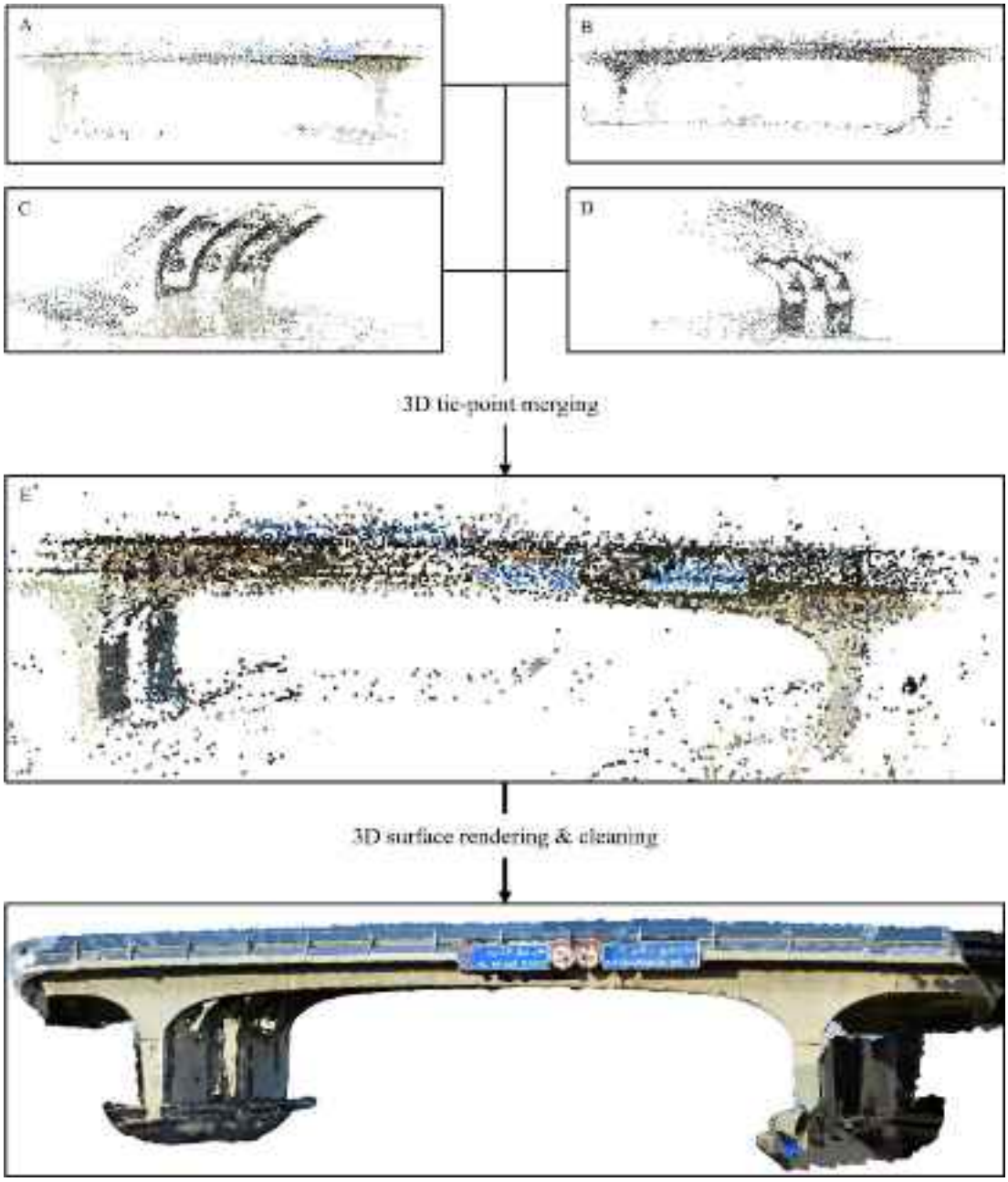

Fig. 7. 3D point clouds of A) front side, B) backside, C) lower left side, D) lower right side, and E) bridge model after merging. F) 3D surface model of the bridge structure.

Table 2
Exterior orientation parameters of a sample of ten images in the front side model.

Photo #	X Precision (m)	Y Precision (m)	Z Precision (m)	Omega Precision (deg.)	Phi Precision (deg.)	Largest Residual (pixels)	RMS Residual (pixels)
1	0.0060	0.0036	0.0059	0.0312	0.0224	1.3599	0.6625
2	0.0043	0.0027	0.0036	0.0592	0.0218	2.0938	0.9101
3	0.0053	0.0055	0.0067	0.1086	0.0303	2.0746	1.066
4	0.0044	0.0028	0.0034	0.0579	0.0161	2.0999	0.9075
5	0.0045	0.0027	0.0035	0.0522	0.0209	2.0891	0.8946
6	0.0055	0.0037	0.0049	0.0244	0.0242	2.0181	1.0627
7	0.0064	0.0039	0.0057	0.0302	0.0221	1.9513	1.0739
8	0.0044	0.0030	0.0032	0.0433	0.0202	2.0784	0.8881
9	0.0046	0.0030	0.0039	0.0658	0.0175	2.0947	0.8716
10	0.0044	0.0028	0.0034	0.0524	0.0208	2.0256	0.7804

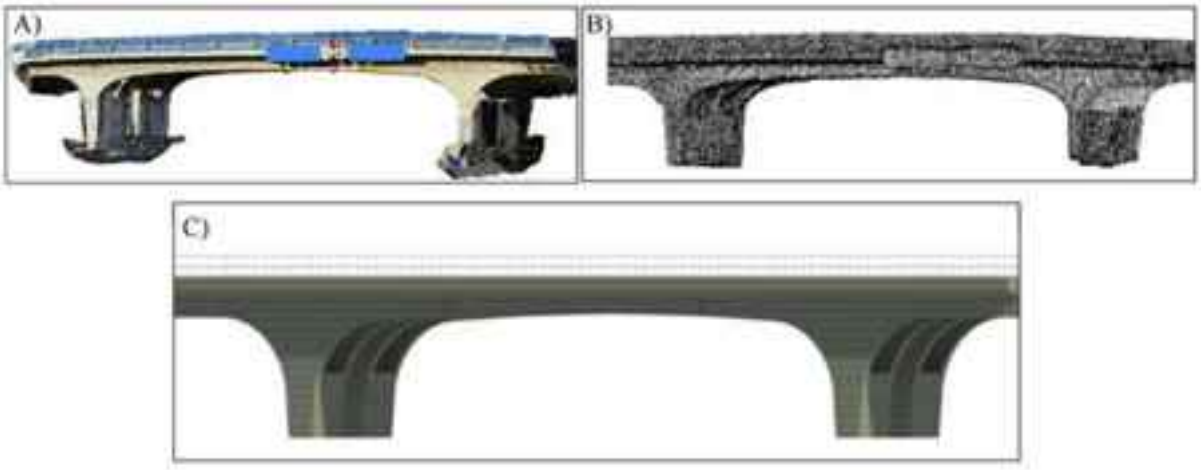

Fig. 8. Generated 3-D model of the bridge A) Photo Modeler 3D Model, B) AutoCAD Model (wireframe), C) Revit 3D Model (textures and materials).

4.1.1. Structural elements modeling

Structural analysis is the typical process for evaluating any bridge's structural condition. The first and most essential steps are documenting a bridge's structure and conducting its geometrical assessment. The complete 3D model obtained after photogrammetric techniques facilitate access to the geometrical information of the bridge's structural components. 3D photogrammetric modeling techniques have become particularly important as measuring instruments for applications in infrastructure, as they can reduce the risks associated with physical access to the structure. In this research, three main geometrical measurements were obtained from the 3D model of the bridge: length, width, and height.

Fig. 9. Perspective View (Revit 3D Model).

In most cases, the original plans and designs of the various bridge infrastructure components are not available, so traditional measurements are required. The traditional modeling methods are therefore used to produce a complete geometrical measurement, which can then be used to generate a two-dimensional drawing. However, the traditional measuring methods that are most commonly employed rely on manual labor and are usually time-consuming and not sufficiently precise. Hence, the photogrammetric model was integrated with CAD modeling to generate an utterly measurable model. These models can either document objects or monitor the actual development of a structure against its designed models.

Additionally, the bridge drawings of the bridge, extracted from the AutoCAD model can facilitate bridge evaluation by bridge inspectors and engineers. Figs. 9 and 10 show the perspective view and the bridge drawings, respectively, with some of the dimensional information in meters extracted from the 3D bridge model. In summary, the parameters evaluated using photogrammetric modeling are the width, length, type, number, orientation, texture, and location of all the deformations.

4.1.2. Model accuracy evaluation

The photogrammetry network control data (GCPs) obtained during data collection is developed to level and scale the 3D point cloud model of the bridge in real space. This 3D similarity transformation analyses the different parameters involving shift, scale, and rotation for the 3D axes (x, y, and z). The completed bridge model comprised 93,881 points cloud; 204 images and 56 well-distributed and identified common GCPs were used through the modeling process. The accuracy of the 3D model and the GCPs attained after processing the data is given in Table 3. This table shows that the GCPs obtained after photogrammetric processing and modeling have an overall RMSE of 0.0035 m and 0.0260 m for the X and Y direction, respectively. While the model has an average tightness of 0.0072 m. The tightness of a point is related to the extent to which the specific light rays intersect. The better and closer they intersect in the 3-D space, the smaller the tightness value. A full 3D geo-referenced textured model is rendered utilizing the restituted point clouds (Fig. 7 F). Furthermore, the framework proposed in this paper is validated by contrasting the measurements obtained from the 3D bridge model with the terrestrial survey measurements. The Z RMSE for this project is fixed coordinates (precision is zero), therefore, not stated in the table.

Dimensional measurements of the different bridge components are identified from the model produced by the photogrammetric software. The three main dimensions of the bridge (length, width, and height) are estimated and compared with the field data col-

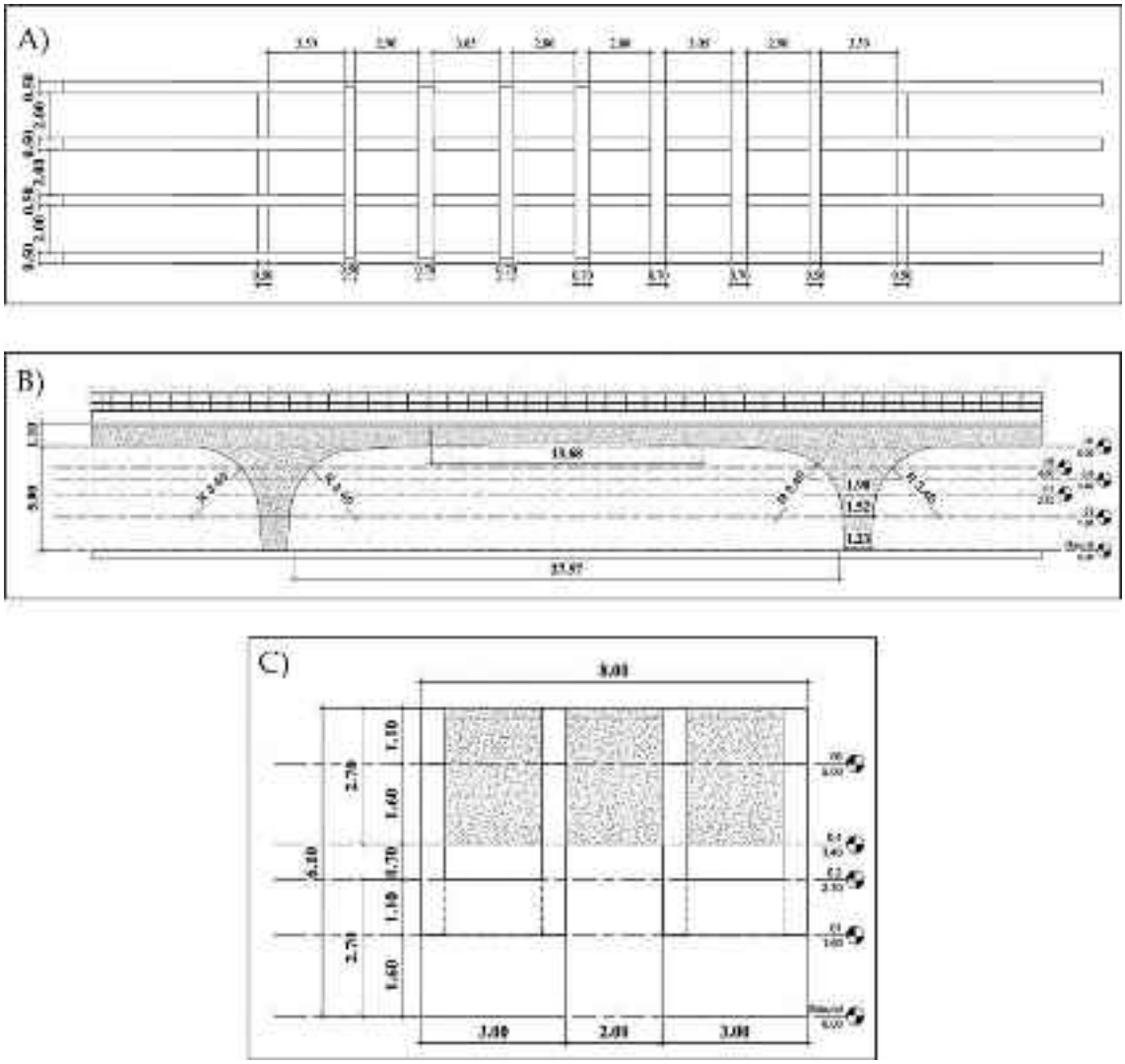

Fig. 10. Bridge drawings with dimensions (in meters), A) Beams framing plan, B) West elevation, C) North elevation.

Table 3
Sample GCPs attained from the field data and the modeling.

ID	X RMSE (m)	Y RMSE (m)	RMS Residual (pixels)	Tightness (m)	Angle (deg.)
1	0.0010	0.0040	0.8612	0.0035	38.2567
9	0.0033	0.0046	0.7561	0.0058	47.6356
11	0.0020	0.0089	0.5269	0.0044	22.5666
14	0.0019	0.0309	0.6741	0.0035	23.7305
16	0.0047	0.0361	1.3289	0.0121	55.8630
17	0.0041	0.0419	0.8461	0.0106	79.2237
23	0.0003	0.0401	0.9821	0.0039	18.8459
26	0.0049	0.0297	1.1445	0.0090	18.1612
29	0.0600	0.0404	1.0634	0.0061	16.6861
30	0.0572	0.0412	0.6822	0.0128	51.9540
Overall RMSE	**0.0035**	**0.0260**	**0.78000**	–	–

lected with the total station (Table 4). The comparison shows that the RMSE of the 3D model ranges from 0.0280 to 0.0880 m.

Finally, the model's overall accuracy was evaluated by comparing the points retrieved for the total station with the PhotoModeler measurements using the point-to-point comparison referring to. Table 5 and Fig. 11 show the measured points and the distance between specific points from different bridge components. This research measured different parameters by selecting several corresponding points on the edge of the bridge surface using coordinate systems X, Y, and Z. The results of the generated model by PhotoModeler indicated that the uncertainty in measurement, as shown in table 5, is ± 0.0041 m. The RMSE of the photogrammetric model is 0.0081 m. The accuracy of the developed model was benchmarked and compared with the literature showed similar results [26,38].

4.2. Bridge defect quantification

Concrete structures such as bridges are exposed to several distresses while in service due to traffic loads, harsh environmental conditions, and traffic accidents, which usually lead to severe damage to the structure and its components. Preventive measures to

Table 4
Measurements of the bridge structure.

Parameter	Total station (m)	PhotoModeler (m)	Error (%)	RMSE (m)	Linear measurement accuracy / Linear Misclosure Length
Length	29.0000	29.1220	0.4200	0.0880	1:239
Width	8.0000	8.0410	0.5100	0.0410	1:197
Height	5.1000	5.1280	0.5500	0.0280	1:183

Table 5
Model accuracy evaluation.

Segment	**Total station coordination**			**PhotoModeler coordination**			Different (m)	Error (%)
	Coordinate 2	Coordinate 1	Distance (m)	Coordinate 2	Coordinate 1	Distance (m)		
S1 (Z_2-Z_1)	356859.8311	356856.9601	2.8710	356859.7922	356856.9143	2.8779	0.0069	0.82
S2 (Z_2-Z_1)	356854.8017	356852.0461	2.7556	356854.8610	356852.1010	2.7600	0.0044	2.27
S3 (Z_2-Z_1)	356866.8313	356852.9300	13.9013	356863.8111	356849.9000	13.9111	0.0098	0.36
S4 (X_2-X_1)	356859.8631	356852.0501	7.8130	356859.8148	356852.0108	7.8040	0.0090	0.39
S5 (Y_2-Y_1)	356853.6642	356845.8197	7.8445	356853.7499	356845.9013	7.8486	0.0041	0.48
RMSE (m)	0.0081							

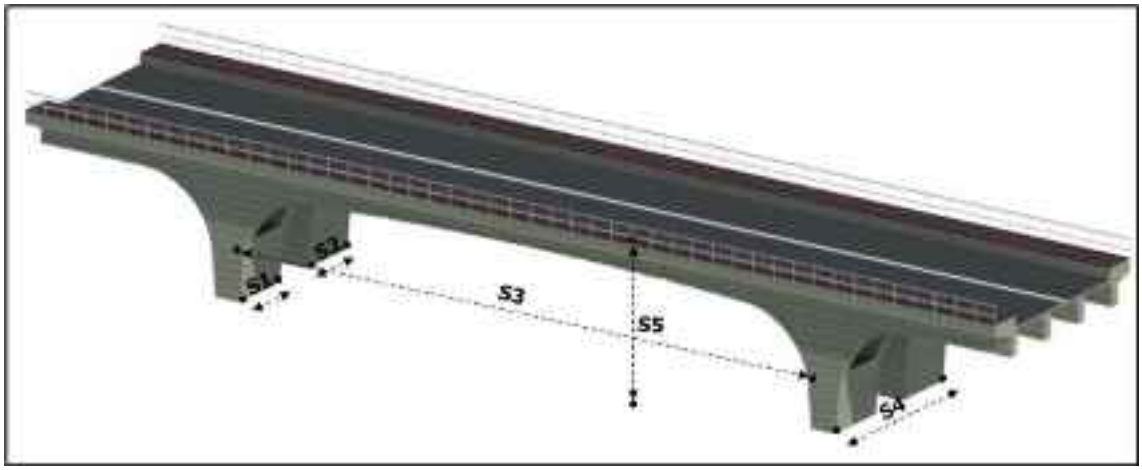

Fig. 11. The obtained segments from the generated model.

minimize damage and failure can be taken if early detection measures are in place [39]. Hence, photogrammetry is implemented for non-destructive bridge defect quantification. The generated 3D photogrammetry model is analyzed with AutoCAD to facilitate extracting information in software commonly used in structural analysis.

The quantification of the substantial damage (concrete) due to an accident where a moving vehicle crashed into the bridge structure is an illustrative example. Fig. 12 shows the bridge section used to estimate the concrete volume loss. The AutoCAD model of the damaged area and its dimensions can be seen in Fig. 13 A and B. The damaged area's length, width, and depth are extracted from the AutoCAD model based on the 3D photogrammetry model. The results indicate that the reduction in the volume of the concrete girder due to this accident is approximately 0.0250 m3 with an accuracy ± 0.0001 m3. In the future, the same method can be used to monitor the level of damage in the bridge.

Cracks in and erosion of the concrete surface of the bridge components are two signs indicating bridges' deterioration and structural degradation. These defects are typically identified and measured manually during visual inspections. The common practice is to capture images of the cracks and manually sketch these on the inspection report during the visual inspection when the conditions for the irregularities are observed and assessed. The main benefit of using the image processing technique for 3D modeling is that it provides more accurate, reliable models than conventional methods. Because the manual analysis depends entirely on the expert's knowledge and experience, this condition assessment lacks objectivity, whereas 3D models that are image-based can provide more accurate interpretations and eliminate subjectivity. Developing a complete 3D model allows for detecting any deformation and provides information about the surface conditions of a bridge.

Fig. 12. The damaged section of the bridge infrastructure shows concrete volume loss.

5. Conclusions and future work

This research work has described the application of an integrated framework methodology combining CRP modeling with geometrical modeling software to generate a complete 3D georeferenced textured model based on bridge images and terrestrial information. The photogrammetric method was utilized for the identification and modeling of existing infrastructure. A reinforced concrete bridge was selected to demonstrate the proposed framework methodology. The bridge selection was based on its condition and age, as well as the fact that there were no bridge drawings of the structure available, making 3D modeling of the bridge a necessity. High-resolution images were captured for use in photogrammetric processing. Four-point cloud models were generated to provide details related to the surface and texture of the bridge. The point cloud models are developed by analyzing high-resolution images collected using a Nikon D4S camera. The images are captured from different positions to provide extensive stereo coverage and maximum overlapping. The images are processed with PhotoModeler software along with the calibration information and GCPs coordinates to create the models. The subsequent steps include 1) bundle adjustment, which assists in identifying the image parameter (location and orientation) within the GCPs, 2) defining a minimum of five tie-points between overlapping images to generate a system of equations that establish the relative external orientation between the images, and 3) generating the points cloud-out-off matching conjugate points. Criteria such as high geometric precision, the detailed availability and efficiency of the model size, and photographic realism were considered during the generation of these models.

This research confirms the feasibility of CRP to create representative 3D models of a bridge that contain all its geometric characteristics and allow for the measurement of the different components and their characteristics. The produced parameters of the bridge model have an accuracy (RMSE 0.0081 m) and uncertainty in the measurement of ± 4.1000 mm. The technological arrangements to develop the bridge information models are simple, available, and can be completed relatively cheaply. In addition, the developed models can capture important details such as damage, cracks, and dimensions, which can be used to assess and monitor the bridge's condition. Furthermore, the developed method can be further evaluated for the potential of assisting bridge inspectors and engineers in evaluating the condition of bridge projects and comparing models created at different times to assess a bridge's aging process.

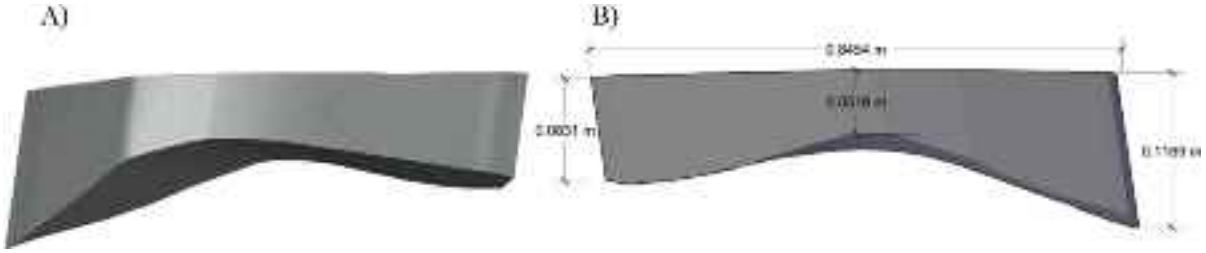

Fig. 13. Fig. A) AutoCAD model and B) Dimensions of the concrete volume missing from the bridge infrastructure.

Developing program scripts using Dynamo or Python to perform analysis of the captured information can be an expansion for future work. Moreover, using the developed model to develop reusable parametric objects for bridges in Revit.

Declaration of Competing Interest

The authors declare that they have no known competing financial interests or personal relationships that could have appeared to influence the work reported in this paper.

Acknowledgment

The authors would like to thank Ministry of Energy and Infrastructure in UAE for facilitating the data collection process and would like to thank Office of Vice Chancellor for Research and Graduate Studies and Research Institute of Sciences and Engineering at University of Sharjah for funding this research study under project number: 19020401133.

References

[1] Rashidi M, Mohammadi M, Kivi SS, Abdolvand MM, Truong-Hong L, Samali B. A decade of modern bridge monitoring using terrestrial laser scanning: Review and future directions. Remote Sens 2020;12:1–34. doi: https://doi.org/10.3390/rs12223796.
[2] Kirk RS, Mallett WJ. Highway bridge conditions: Issues for congress. US Transit, Transp Infrastruct Considerations Dev 2014;5:49–68.
[3] Hooks J, Frangopol DM. LTBP bridge performance primer. US Bridg Cond Long-Term Bridg Perform A Prim 2014:21–89.
[4] Abu Dabous S, Alkass S. A stochastic method for condition rating of concrete bridges. Constr. Res. Congr. 2010 Innov. Reshaping Constr. Pract. - Proc. 2010 Constr. Res. Congr., vol. 41109, 2010, p. 558–67. 10.1061/41109(373)56.
[5] Abu Dabous S, Al-Khayyat G. A Flexible bridge rating method based on Analytical Evidential Reasoning and Monte Carlo Simulation. Adv. Civ. Eng. 2018:1290632. doi: https://doi.org/10.1155/2018/1290632.
[6] Mohamed Mansour DM, Moustafa IM, Khalil AH, Mahdi HA. An assessment model for identifying maintenance priorities strategy for bridges. Ain Shams Eng J 2019;10:695–704. doi: https://doi.org/10.1016/j.asej.2019.06.003.
[7] Street NC. THE MANUAL FOR BRIDGE EVALUATION 2019 Interim Revisions 2018.
[8] Access E, Summary E, Bridge N, Standards I. 61494 Agency : National Bridge Inspection Standards. Fed Highw Adm (FHWA). US 2019;84:61494–516.
[9] Division C, Llc A. Bridge Deterioration Models and Rates 2020.
[10] Chantrelle FP, Lahmidi H, Keilholz W, El MM, Michel P. Development of a multicriteria tool for optimizing the renovation of buildings. Appl Energy 2011;88:1386–94. doi: https://doi.org/10.1016/j.apenergy.2010.10.002.
[11] Abu Dabous S, Alkass S. Managing bridge infrastructure under budget constraints: A decision support methodology. Can J Civ Eng 2011;38:1227–37. doi: https://doi.org/10.1139/l11-082.
[12] Truong-hong L, Hinks T, Carr H. Combining an Angle Criterion with Voxelization and the Flying Voxel Method in Reconstructing Building Models from LiDAR Data. Comput Civ Infrastruct Eng 2012;00:1–18. doi: https://doi.org/10.1111/j.1467-8667.2012.00761.x.
[13] Dizaji MS, Harris DK, Kassner B, Hill JC. Full-field non-destructive image-based diagnostics of a structure using 3D digital image correlation and laser scanner techniques. J Civ Struct Heal Monit 2021;11:1415–28. doi: https://doi.org/10.1007/s13349-021-00516-6.
[14] Eschmann C, Wundsam T. Web-Based Georeferenced 3D Inspection and Monitoring of Bridges with Unmanned Aircraft Systems. J Surv Eng 2017;143:1–10. doi: https://doi.org/10.1061/(ASCE)SU.1943-5428.0000221.
[15] Zhang C, Elaksher A. An Unmanned Aerial Vehicle-Based Imaging System for 3D Measurement of Unpaved Road. Comput Civ Infrastruct Eng 2012;27:118–29. doi: https://doi.org/10.1111/j.1467-8667.2011.00727.x.
[16] Ma Y, Zheng Y, Cheng J, Easa S. Real-Time Visualization Method for Estimating 3D Highway Sight Distance Using LiDAR Data. J Transp Eng Part A Syst 2019;145:1–14. doi: https://doi.org/10.1061/JTEPBS.0000228.
[17] Yeum CM, Choi J, Dyke SJ. Automated region-of-interest localization and classification for vision-based visual assessment of civil infrastructure. Struct Heal Monit 2019;18:675–89. doi: https://doi.org/10.1177/1475921718765419.
[18] Zhou Z, Gong J, Guo M. Image-Based 3D Reconstruction for Posthurricane Residential Building Damage Assessment. J Comput Civ Eng 2016:30. doi: https://doi.org/10.1061/(ASCE)CP.1943-5487.0000480.
[19] Maas H, Hampel U. Photogrammetric Techniques in Civil Engineering Material Testing and Structure Monitoring. Photogramm Eng Remote Sens 2006;1:39–45. 10.14358/PERS.72.1.39.
[20] Alemdar ZF, Browning JA, Olafsen J. Photogrammetric measurements of RC bridge column deformations. Eng Struct 2013;33:2407–15. doi: https://doi.org/10.1016/j.engstruct.2011.04.015.
[21] Abu Dabous S, Feroz S. Condition monitoring of bridges with non-contact testing technologies. Autom Constr 2020;116:. doi: https://doi.org/10.1016/j.autcon.2020.103224103224.
[22] Hu J, Liu E, Yu J. Application of Structural Deformation Monitoring Based on Close-Range Photogrammetry Technology. Adv. Civ Eng 2021; 2021.. doi: https://doi.org/10.1155/2021/6621440.
[23] Kwiatkowski J, Anigacz W, Beben D. Comparison of Non-Destructive Techniques for Technological Bridge Deflection Testing. Materials (Basel) 2020:1–16. 10.3390/ma13081908.
[24] Belloni V, Sjölander A, Ravanelli R, Crespi M, Nascetti A. Tack Project: Tunnel and Bridge Automatic Crack Monitoring Using Deep Learning and Photogrammetry. ISPRS - Int Arch Photogramm Remote Sens Spat Inf Sci 2020;XLIII-B4-2:741–5. 10.5194/isprs-archives-xliii-b4-2020-741-2020.
[25] Mohammadi M, Rashidi M, Mousavi V, Karami A, Yu Y, Samali B. Case study on accuracy comparison of digital twins developed for a heritage bridge via UAV photogrammetry and terrestrial laser scanning. Int Conf Struct Heal Monit Intell Infrastruct Transf Res into Pract SHMII 2021;2021-June:1713–20.
[26] Mohammadi M, Rashidi M, Mousavi V, Karami A, Yu Y, Samali B. Quality evaluation of digital twins generated based on uav photogrammetry and tls: Bridge case study. Remote Sens 2021;13:1–22. doi: https://doi.org/10.3390/rs13173499.
[27] Jiang R, Jauregui DV. Development of a digital close-range photogrammetric bridge deflection measurement system. Meas J Int Meas Confed 2010;43:1431–8. doi: https://doi.org/10.1016/j.measurement.2010.08.015.
[28] Jáuregui D V., White KR, Woodward CB, Leitch KR. Noncontact photogrammetric measurement of vertical bridge deflection. J Bridg Eng 2013;8:212–22. 10.1061/(ASCE)1084-0702(2003)8:4(212).
[29] Zhang G, Guo G, Li L, Yu C. Study on the dynamic properties of a suspended bridge using monocular digital photography to monitor the bridge dynamic deformation. J Civ Struct Heal Monit 2018;8:555–67. doi: https://doi.org/10.1007/s13349-018-0293-4.
[30] Arias P, Ordonez C, Lorenzo H, Herraez J, Armesto J. Low-cost documentation of traditional agro-industrial buildings by close-range photogrammetry. Build Environ 2007;42:1817–27. doi: https://doi.org/10.1016/j.buildenv.2006.02.002.
[31] Atkinson KB. Close Range Photogrammetry and Machine Vision. Whittles Publishing; 1996.
[32] Dedei Tagoe N, Mantey S. Determination of the Interior Orientation Parameters of a Non-metric Digital Camera for Terrestrial Photogrammetric Applications. Ghana Min J 2019;19:1–9. doi: https://doi.org/10.4314/gm.v19i2.1.
[33] Jáuregui D V., White KR. Bridge inspection using virtual reality and photogrammetry. Woodhead Publishing Limited; 2005. 10.1533/9781845690953.216.
[34] Sánchez-Aparicio LJ, Herrero-Huerta M, Esposito R, Schipper HR, González-Aguilera D. Photogrammetric solution for analysis of out-of-plane movements of a masonry structure in a large-scale laboratory experiment. Remote Sens 2019:11. doi: https://doi.org/10.3390/rs11161871.
[35] Chen T, Shibasaki R, Lin Z. A rigorous laboratory calibration method for interior orientation of an airborne linear push-broom camera. Photogramm Eng Remote Sensing 2007;73:369–74. 10.14358/PERS.73.4.369.
[36] Xu Y. Photogrammetry-based structural damage detection by tracking a visible laser line. Struct Heal Monit 2020;19:322–36. doi: https://doi.org/10.1177/1475921719840354.
[37] Riveiro B, Jauregui DV, Arias P, Armesto J, Jiang R. An innovative method for remote measurement of minimum vertical underclearance in routine bridge inspection. Autom Constr 2012;25:34–40. doi: https://doi.org/10.1016/j.autcon.2012.04.008.
[38] Mohammadi M, Rashidi M, Mousavi V, Yu Y, Samali B. Application of TLS Method in Digitization of Bridge Infrastructures: A Path to Br IM Development. Remote Sens 2022:14. doi: https://doi.org/10.3390/rs14051148.
[39] Henke K, Pawlowski R, Schregle P, Winter S. Use of digital image processing in the monitoring of deformations in building structures. J Civ Struct Heal Monit 2015;5:141–52. doi: https://doi.org/10.1007/s13349-014-0091-6.